

# Communication: Growing room temperature ice with graphene

Cite as: J. Chem. Phys. **138**, 121101 (2013); <https://doi.org/10.1063/1.4798941>

Submitted: 08 January 2013 . Accepted: 19 March 2013 . Published Online: 28 March 2013

Albert Verdaguer, Juan José Segura, Laura López-Mir, Guillaume Sauthier, and Jordi Fraxedas



View Online



Export Citation



CrossMark

## ARTICLES YOU MAY BE INTERESTED IN

[The environment of graphene probed by electrostatic force microscopy](#)

Applied Physics Letters **92**, 123507 (2008); <https://doi.org/10.1063/1.2898501>

[Coarsening dynamics of ice crystals intercalated between graphene and supporting mica](#)

Applied Physics Letters **108**, 011601 (2016); <https://doi.org/10.1063/1.4939188>

[First-principles studies of water adsorption on graphene: The role of the substrate](#)

Applied Physics Letters **93**, 202110 (2008); <https://doi.org/10.1063/1.3033202>

The Journal  
of Chemical Physics

Submit Today

The Emerging Investigators Special Collection and Awards  
Recognizing the excellent work of early career researchers!



## Communication: Growing room temperature ice with graphene

Albert Verdager,<sup>1,a)</sup> Juan José Segura,<sup>2</sup> Laura López-Mir,<sup>1</sup> Guillaume Sauthier,<sup>1</sup> and Jordi Fraxedas<sup>1,b)</sup>

<sup>1</sup>Centre d'Investigació en Nanociència i Nanotecnologia, CIN2 (CSIC-ICN), Edifici CM7, Campus UAB, E-08193 Barcelona, Catalunya, Spain

<sup>2</sup>Institute of Materials, École Polytechnique Fédérale de Lausanne, CH-1015 Lausanne, Switzerland

(Received 8 January 2013; accepted 19 March 2013; published online 28 March 2013)

Water becomes ordered in the form of hexagonal ice at room temperature under controlled humidity conditions upon confinement in the nanometer range between protective graphene sheets and crystalline (111) surfaces with hexagonal symmetry of the alkali earth fluoride BaF<sub>2</sub>. Interfacial water/substrate pseudoepitaxy turns out to be a critical parameter since ice is only formed when the lattice mismatch is small, an observation based on the absence of ice on (111) surfaces of isostructural CaF<sub>2</sub> © 2013 American Institute of Physics. [<http://dx.doi.org/10.1063/1.4798941>]

When water becomes spatially confined between two parallel surfaces separated by distances comparable to the water mean molecular diameter ( $\sim 0.28$  nm), the structural isotropy characteristic of bulk water is lost and water becomes layered.<sup>1–4</sup> Such layering effect has been experimentally evidenced recently by means of scanning probe microscopy measurements using protective graphene sheets as one of the confining surfaces.<sup>5–8</sup> When graphene sheets are deposited on cleaved mica surfaces in ambient conditions, room temperature (RT), and controlled relative humidity (RH), the trapped water layers grow in a two dimensional (2D) mode, forming atomically flat structures with heights of 0.37 nm, the distance between adjacent bilayers (BLs) in hexagonal ice (Ih).

The same 2D growth has been observed using highly oriented pyrolytic graphite (HOPG)<sup>9</sup> and sapphire<sup>10</sup> substrates. The observed BL structure corresponds to the commonly accepted structure for the first water monolayer (ML) on many surfaces.<sup>11,12</sup> The fact that 0.37 nm high water layers are observed on different surfaces with very different affinity to water draws the attention towards the role of the water/graphene interface. On SiO<sub>2</sub>, despite the fact that the presence of ice Ih BLs has been suggested<sup>13</sup> no such structures have been observed when using graphene.<sup>5</sup> The similitude in the measured heights on different surfaces has been ascribed to the reorganization of hydrogen bonding induced by the hydrophobic graphene sheet.<sup>10</sup>

Note that the ice Ih BL structure is formed at RT, so that the term RT ice is fully justified. RT ice can be also prepared by applying external pressures, although in crystal structures different from ice Ih. Above 2 GPa, ice VII is formed and well above such value, at 65.8 GPa, another polymorph (ice X) is obtained.<sup>14</sup> Ice has been imaged at RT with an atomic force microscope (AFM) in contact mode (c-AFM)<sup>15</sup> and using a friction force microscope<sup>16</sup> on cleaved HOPG surfaces in air, in spite of its hydrophobic character. The viscoelastic response of confined water has been also studied with an AFM.<sup>17</sup> In this case the elastic (solid-like) and viscous

(liquid-like) response oscillates with molecular layering as the tip-surface gap is reduced, corresponding to short-range ordering of the water in the tip-surface gap.<sup>18</sup> In addition, a stepwise behavior with a periodicity of about 0.25 nm has been observed using a shear force microscope.<sup>19</sup>

In this work, we have studied the combined effect of graphene and cleaved surfaces of alkali earth fluorides with hexagonal symmetry at ambient conditions on the structuration of water into RT ice. We have used single crystalline isostructural BaF<sub>2</sub> and CaF<sub>2</sub>(111) substrates (*Fm* $\bar{3}$ *m* space group) because of their differentiated surface lattice constants, 0.438 and 0.384 nm, respectively, which are to be compared to the surface lattice constant of the basal plane of ice Ih (0.45117 nm at 223 K<sup>20</sup>). The results shown here evidence that water layers confined between graphene sheets and BaF<sub>2</sub>(111) surfaces are highly structured and compatible with an ice Ih structure, as opposed to previous AFM experiments performed on free BaF<sub>2</sub>(111) surfaces (without protective graphene sheets)<sup>21–24</sup> and to theoretical calculations.<sup>25</sup> This suggests a strong effect of the graphene sheet on the structure of the trapped water films. However, water is not structured on CaF<sub>2</sub>(111) surfaces indicating that the interaction between water molecules and the substrate is also playing an important role.

Graphene sheets were transferred through the standard method of mechanical exfoliation of Kish graphite flakes<sup>26</sup> onto freshly cleaved (111) BaF<sub>2</sub> and CaF<sub>2</sub> surfaces inside a glove box at controlled RH.<sup>21</sup> The samples were then studied using an Agilent 5500 and an MFP-3D Asylum Research AFM at ambient conditions. Large areas were scanned using the amplitude modulation (AM-AFM) mode and the water layers trapped between graphene sheets and crystal surfaces were imaged in c-AFM mode using the same cantilever tip (PPP-FMR and PPP-EFM from Nanosensors) with typical resonance frequencies of 70 kHz and force constants of 2 N/m.

In Fig. 1(a), a large AM-AFM image of few nm thick (few layer) graphene sheets deposited at  $\sim 30\%$  RH on a freshly cleaved BaF<sub>2</sub>(111) surface is shown. Substrate steps are observed under the graphene sheets evidencing the

<sup>a)</sup>Electronic mail: averdager@cin2.cat.

<sup>b)</sup>Electronic mail: jfraxedas@cin2.cat.

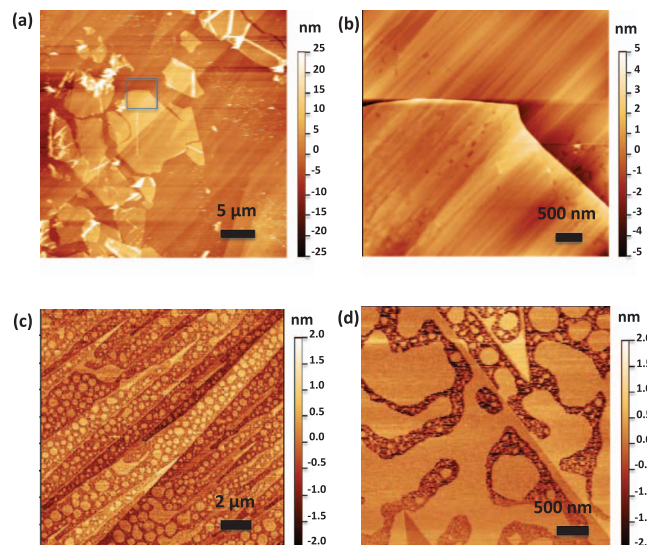


FIG. 1. (Top) Freshly cleaved  $\text{BaF}_2(111)$  surface partially covered with few layer graphene flakes deposited at 30% RH. (a) AM-AFM and (b) c-AFM images taken at RT. Bright stripes in (a) correspond to graphene wrinkles. The image in (b) corresponds to a magnified view of the area enclosed in the square in (a). (Bottom) AM-AFM images taken at 50% RH and RT of a freshly cleaved  $\text{BaF}_2(111)$  surface covered with water layers corresponding to the (c) unperturbed and (d) perturbed case, respectively.

capability of measuring structures below few layer graphene sheets. A detailed look in Fig. 1(b), taken in c-AFM mode and corresponding to the area enclosed in the square in Fig. 1(a), reveals the characteristic V-shaped step structure of the surface.<sup>22</sup> The measured step height is  $0.35 \pm 0.02$  nm for both the free and covered surfaces, a value that corresponds to the distance between adjacent trilayer planes (0.36 nm according to the known crystallographic structure), thus almost identical to the water 0.37 nm interbilayer distance. In the covered regions noticeable changes are observed due to the presence of water, trapped by the graphene during the deposition procedure. The observed water-induced structures are rather stable. When such surfaces are exposed to RH cycles of low RH ( $<10\%$ ), high RH ( $\sim 80\%$ ), and back to low RH no significant modifications are observed, contrary to recently reported experiments.<sup>6</sup>

We compare the c-AFM image with AM-AFM images for freshly cleaved free  $\text{BaF}_2(111)$  surfaces at RH  $\sim 50\%$  in Figs. 1(c) and 1(d). Both figures correspond to intentionally unperturbed and perturbed surfaces by the controlled action of the oscillating tip, respectively.<sup>24</sup> Using nonperturbative real non-contact AM-AFM in ambient conditions rounded water patches on terraces<sup>21,24</sup> and water ribbons and menisci decorating the steps<sup>22</sup> are observed with heights in the 0.5–1 nm range at  $20 < \text{RH} < 60\%$ . Thus, the unconfined structures are morphologically different and exhibit different heights as compared to the layered structures observed for water confined between  $\text{BaF}_2(111)$  surfaces and a graphene sheet.

The confined structures depend on the RH at which the graphene sheets were deposited. In Fig. 2, c-AFM images of graphene sheets deposited on freshly cleaved  $\text{BaF}_2(111)$  surfaces at different RHs are shown. Even at very low humidity (RH  $< 10\%$ ) small patches of water can be observed specially along the steps. At 15% RH, a well-defined lay-

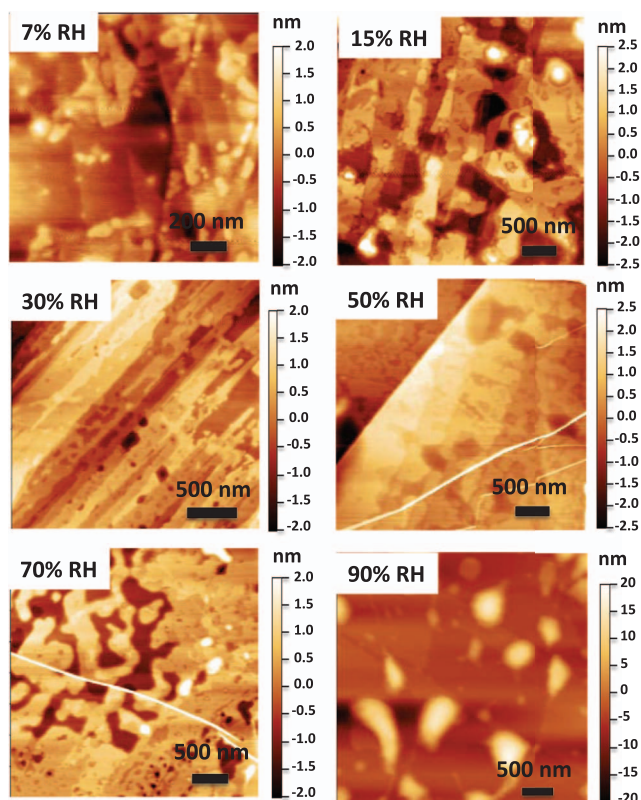


FIG. 2. c-AFM images of few layer graphene deposited on freshly cleaved  $\text{BaF}_2(111)$  surfaces at 7%, 15%, 30%, 50%, 70%, and 90% RH, respectively. Bright stripes correspond to graphene wrinkles.

ered structure covers most of the substrate surface. The layers are flat and limited by well-defined step edges and still reveal the underlying  $\text{BaF}_2$  step structure. No remarkable differences are observed for samples prepared at 15%, 30%, and 50% RH. The layers observed for the sample prepared at 50% RH are of particular interest. In this case the low density of steps of the cleaved  $\text{BaF}_2(111)$  surface allows a better investigation of the water layers and the interaction with steps, as will be discussed below. At 70% RH multilayers are observed on the surface showing rounded edges with a well-defined layer-by-layer structure. Finally, at 90% RH a thick homogeneous film is observed with trapped tens of nm high water droplets.

Figure 3(a) shows a c-AFM image (zoom of Fig. 2 corresponding to 50% RH) together with a cross section line profile and a height distribution histogram plots. We observe that water layers cover the terraces limited by the triangular steps and that two different heights are observed,  $0.36 \pm 0.03$  and  $0.25 \pm 0.03$  nm, for the water layers. The first one is practically identical to the intrinsic  $\text{BaF}_2(111)$  step height (0.36 nm), which can be used as an internal height reference because it corresponds to the distance between adjacent trilayers of the solid. The 0.36 nm water layers are in line with the presence of an ice Ih BL since the Ih interbilayer distance is  $c/2 = 0.37$  nm, where  $c$  stands for the lattice constant of ice Ih along the direction perpendicular to the basal plane.

Let us now discuss on the twofold structuring character that the water molecules sense when sandwiched between both surfaces. Water molecules on  $\text{BaF}_2(111)$  surfaces

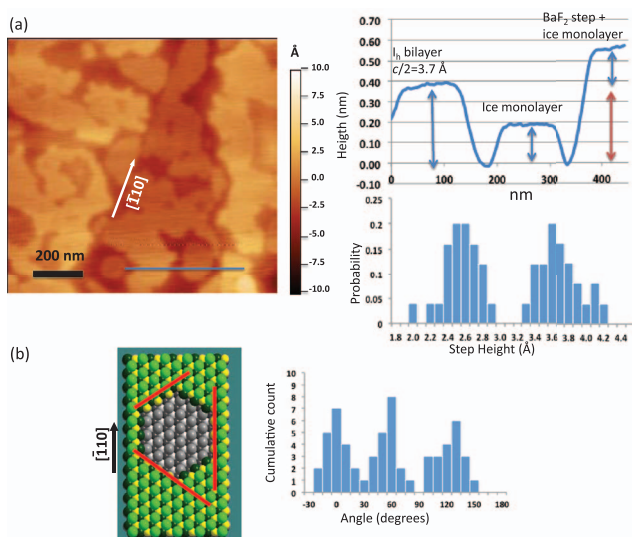


FIG. 3. (a) (left) c-AFM image of few layer graphene deposited on freshly cleaved BaF<sub>2</sub>(111) surfaces at 50% RH (as in Fig. 2), where the crystallographic  $[\bar{1}10]$  direction is indicated. (Top right) Cross section of the line drawn in the image and (bottom right) histogram of the distribution of heights. (b) (left) Scheme of the (111) surface showing the main directions (in red) corresponding to the angles 0°, 60°, and 120° referred to  $[\bar{1}10]$  extracted from the histogram (right).

exposed to the atmosphere have a high diffusion according to AFM<sup>22</sup> and infrared<sup>27</sup> experiments and density functional theory (DFT)<sup>28</sup> calculations and become trapped at defects such as vacancies and steps. The effect of the graphene is to efficiently limit such mobility on the surface allowing for 2D nucleation and growth, emulating the effect of low temperatures in a vacuum. On the other hand graphene hinders any displacement out of the surface. Graphene is hydrophobic, exhibiting contact angles as high as 127°,<sup>29</sup> but it has been shown that water adsorbs on it when deposited on SiO<sub>2</sub> acting as a discharging agent<sup>30,31</sup> and showing some transparency to van der Waals interactions.<sup>32</sup> In aqueous media water is highly structured on the graphene surface, which has been attributed to the distribution of hydrogen bonds at the interface.<sup>33,34</sup> Thus, the combined effect of both surfaces eliminates one degree of freedom (perpendicular to the interface), forces the saturation of hydrogen bonds (graphene), and triggers nucleation (substrate). This would explain the coverage observed at RH as low as 15%. Actually, a coverage of half of a ML is already expected at 15% RH according to isotherms calculated from infrared measurements.<sup>27</sup>

The 0.25 nm high features are of the order of the mean molecular diameter, suggesting that the molecules lie flat on the interface. Such a configuration is compatible with a cross-linked structure in which all water molecules are at the same vertical position (i.e., no BL is formed).<sup>25</sup> In this case the interaction with the substrate is strong enough to avoid the formation of ice Ih BLs probably caused by a local lower density. Surface potential measurements performed at RT indicate the unlikelihood of the formation of ice Ih BLs on the free BaF<sub>2</sub>(111) surface<sup>21</sup> so that probably both configurations, cross-linked and ice Ih BL, coexist at the interface.

An analysis of the angular distribution of the water layer edges with respect to the crystallographic  $[\bar{1}10]$  direction, de-

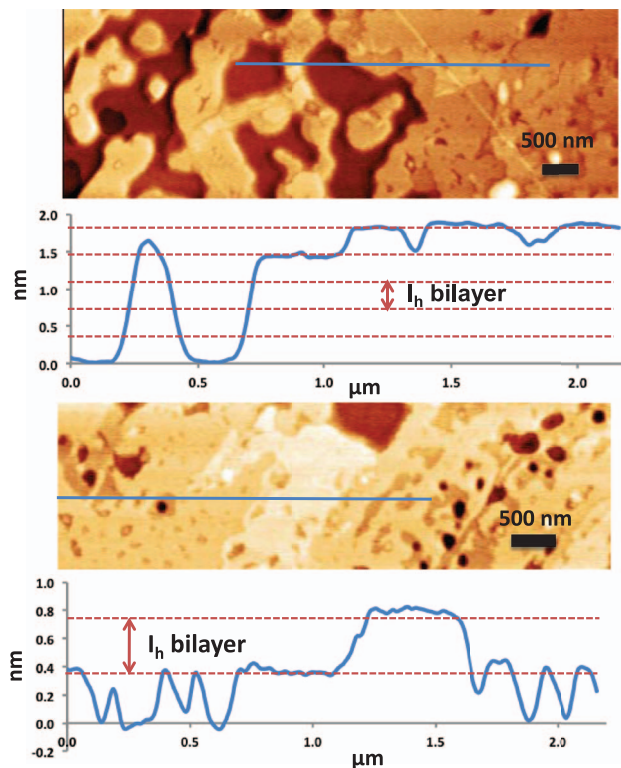


FIG. 4. Height profiles of two different regions of the c-AFM image from Fig. 2 (sample prepared at RH  $\sim$  70%). The images have been slightly shaded in order to enhance the contrast at water layers edges. Discontinuous parallel lines indicate the expected location of ice Ih BLs and the interbilayer distance (0.37 nm).

finied by one of the steps in Fig. 3(a), is shown in Fig. 3(b) (right). The distribution is centered at about 0°, 60°, and 120°, indicating a clear directionality induced by the hexagonal symmetry of the substrate as previously shown on uncovered mica surfaces.<sup>35</sup>

It is interesting to observe that the layered structure is maintained when more water layers are adsorbed on the surface. This is illustrated in Fig. 4 where two regions from the 70% RH case of Fig. 2 are shown together with their corresponding height profiles. From the cross sections we observe that the layers are integer multiples of  $\approx 0.37$  nm.

The comparison with CaF<sub>2</sub>(111) is quite revealing. BaF<sub>2</sub> and CaF<sub>2</sub> are isostructural and water molecules adsorb on their (111) surface with similar binding energies and diffusion barriers<sup>28</sup> but due to the difference in the lattice mismatch with the basal plane of ice Ih water adlayers at both nanometer and macroscopic level are very different on both surfaces.<sup>23</sup> Water trapped between graphene and CaF<sub>2</sub>(111) shows very different structures as compared to BaF<sub>2</sub> as it can be observed in Fig. 5. Water patches exhibit rounded edges with thickness in the order of 1 nm. No water patches of 0.37 nm or 0.25 nm have been observed indicating the absence of ice Ih structures on CaF<sub>2</sub>. The observed structures remind the water layers observed with AM-AFM techniques after perturbation with the cantilever tip [see Fig. 1(d)]. In the CaF<sub>2</sub>(111) case the results indicate that graphene interaction with the water molecules is not sufficient to induce the formation of ice-like structures.

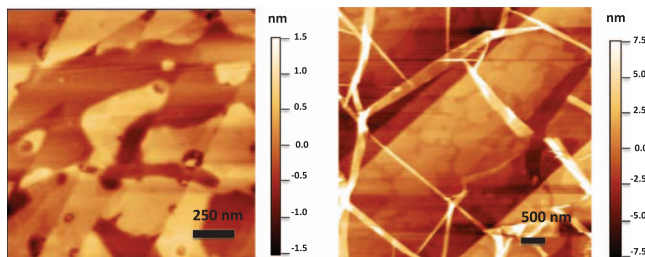


FIG. 5. c-AFM images of few layer graphene on  $\text{CaF}_2(111)$  (left) and  $\text{BaF}_2(111)$  (right) prepared at 40% RH. Bright stripes correspond to graphene wrinkles.

In summary, we have deposited few layer graphene films on freshly cleaved (111) surfaces of  $\text{BaF}_2$  and  $\text{CaF}_2$  single crystals in controlled humidity conditions. Atmospheric water becomes sandwiched and confined between both surfaces. In the case of  $\text{BaF}_2$  water BLs are built compatible with the ice Ih structure, given their height (0.37 nm), as well as multilayers for humidities above 50%. 0.25 nm high features are also observed which might correspond to a cross-linked distribution, so that both configurations (ice Ih and cross-linked) coexist at the graphene/ $\text{BaF}_2(111)$  interface. However, such ordered structure is not observed for  $\text{CaF}_2$ , with exhibits a large lattice mismatch with respect to ice Ih. We conclude that ice Ih at room temperature is grown by the combined effect of the substrate and graphene provided that lattice registry is met.

This work was in part supported by the Ministerio de Ciencia e Innovación (MICINN), Spain, through Project Nos. FIS2009-08355 and MAT2011-23712. J.J.S. thanks the Consejo Superior de Investigaciones Científicas (CSIC) for a JAE DOC Ph.D. grant. Thanks are due to N. Domingo for helping in the experimental setup.

<sup>1</sup>J. N. Israelachvili and R. M. Pashley, *Nature (London)* **306**, 249 (1983).

<sup>2</sup>J. N. Israelachvili, *Intermolecular and Surface Forces* (Academic Press, London, 1991).

<sup>3</sup>I. Brovchenko and A. Oleinova, *Interfacial and Confined Water* (Elsevier, 2008).

<sup>4</sup>T. G. Lombardo, N. Giovambattista, and P. G. Debenedetti, *Faraday Discuss.* **141**, 359 (2009).

<sup>5</sup>K. Xu, P. Cao, and J. R. Heath, *Science* **329**, 1188 (2010).

<sup>6</sup>N. Severin, P. Lange, I. M. Sokolov, and J. P. Rabe, *Nano Lett.* **12**, 774 (2012).

<sup>7</sup>X. Feng, S. Maier, and M. Salmeron, *J. Am. Chem. Soc.* **134**, 5662 (2012).

<sup>8</sup>K. T. He, J. D. Wood, G. P. Doidge, E. Pop, and J. W. Lyding, *Nano Lett.* **12**, 2665 (2012).

<sup>9</sup>P. G. Cao, K. Xu, J. O. Varghese, and J. R. Heath, *Nano Lett.* **11**, 5581 (2011).

<sup>10</sup>H. Komurasaki, T. Tsukamoto, K. Yamazaki, and T. Ogino, *J. Phys. Chem. C* **116**, 10084 (2012).

<sup>11</sup>A. Verdaguer, G. M. Sacha, H. Bluhm, and M. Salmeron, *Chem. Rev.* **106**, 1478 (2006).

<sup>12</sup>P. J. Feibelman, *Phys. Today* **63**(2), 34 (2010).

<sup>13</sup>A. Verdaguer, C. Weis, G. Oncins, G. Ketteler, H. Bluhm, and M. Salmeron, *Langmuir* **23**, 9699 (2007).

<sup>14</sup>E. A. Zheligoyskaya and G. G. Malenkov, *Russ. Chem. Rev.* **75**, 57 (2006).

<sup>15</sup>O. Teschke, *Langmuir* **26**, 16986 (2010).

<sup>16</sup>K. B. Jinesh and J. W. M. Frenken, *Phys. Rev. Lett.* **101**, 036101 (2008).

<sup>17</sup>J. Fraxedas, A. Verdaguer, F. Sanz, S. Baudron, and P. Batail, *Surf. Sci.* **588**, 41 (2005).

<sup>18</sup>S. H. Khan, G. Matei, S. Patil, and P. M. Hoffmann, *Phys. Rev. Lett.* **105**, 106101 (2010).

<sup>19</sup>M. Antognozzi, A. D. L. Humphris, and M. J. Miles, *Appl. Phys. Lett.* **78**, 300 (2001).

<sup>20</sup>K. Röttger, A. Endriss, J. Ihringer, S. Doyle, and W. F. Kuhs, *Acta Crystallogr. B* **50**, 644 (1994).

<sup>21</sup>A. Verdaguer, M. Cardellach, and J. Fraxedas, *J. Chem. Phys.* **129**, 174705 (2008).

<sup>22</sup>M. Cardellach, A. Verdaguer, J. Santiso, and J. Fraxedas, *J. Chem. Phys.* **132**, 234708 (2010).

<sup>23</sup>M. Cardellach, A. Verdaguer, and J. Fraxedas, *Surf. Sci.* **605**, 1929 (2011).

<sup>24</sup>S. Santos, A. Verdaguer, T. Souier, N. H. Thomson, and M. Chiesa, *Nanotechnology* **22**, 465705 (2011).

<sup>25</sup>D. R. Nutt and A. J. Stone, *J. Chem. Phys.* **117**, 800 (2002).

<sup>26</sup>K. S. Novoselov, D. Jiang, F. Schedin, T. J. Booth, V. V. Khotkevich, S. V. Morozov, and A. K. Geim, *Proc. Natl. Acad. Sci. U.S.A.* **102**, 10451 (2005).

<sup>27</sup>V. Sadtschenko, P. Conrad, and G. E. Ewing, *J. Chem. Phys.* **116**, 4293 (2002).

<sup>28</sup>A. S. Foster, T. Trevethan, and A. L. Shluger, *Phys. Rev. B* **80**, 115421 (2009).

<sup>29</sup>S. R. Wang, Y. Zhang, N. Abidi, and L. Cabrales, *Langmuir* **25**, 11078 (2009).

<sup>30</sup>J. Moser, A. Verdaguer, D. Jimenez, A. Barreiro, and A. Bachtold, *Appl. Phys. Lett.* **92**, 123507 (2008).

<sup>31</sup>A. Verdaguer, M. Cardellach, J. J. Segura, G. M. Sacha, J. Moser, M. Zdrojek, A. Bachtold, and J. Fraxedas, *Appl. Phys. Lett.* **94**, 233105 (2009).

<sup>32</sup>J. Rafiee, X. Mi, H. Gullapalli, A. V. Thomas, F. Yavari, Y. Shi, P. M. Ajayan, and N. A. Koratkar, *Nature Mater.* **11**, 217 (2012).

<sup>33</sup>D. Chandler, *Nature (London)* **437**, 640 (2005).

<sup>34</sup>K. Suzuki, N. Oyabu, K. Kobayashi, K. Matsushige, and H. Yamada, *Appl. Phys. Express* **4**, 125102 (2011).

<sup>35</sup>J. Hu, X. D. Xiao, D. F. Ogletree, and M. Salmeron, *Science* **268**, 267 (1995).